PNAS RESEARCH ARTICLE | GENETICS

HairTime: A noninvasive assay for estimating circadian phase from a single hair sample

Bert Maier[a,1], Luísa K. Pilz[b,c,1], Selin Özcakir[a,1], Ali Rahjouei[b], Ashraf N. Abdo[a,2], Jan de Zeeuw[d,e], Dieter Kunz[d,e], and Achim Kramer[a,3]

Affiliations are included on p. 11.

Edited by Ravi Allada, University of Michigan, Ann Arbor, MI; received June 9, 2025; accepted February 20, 2026 by Editorial Board Member Michael Rosbash

Circadian clocks govern daily physiological and behavioral processes and are crucial for health; disruptions can lead to various diseases. The circadian phase of entrainment—the phase of the internal circadian clock in relation to external environmental cycles—is influenced by both genetic and environmental factors, varies between individuals, and is reflected in daily behaviors such as sleep–wake patterns, cognitive performance, and physical activity. While circadian phase may also fluctuate within individuals, the dynamics and extent of such variation in daily life remain largely unexplored. The gold standard for circadian phase assessment, dim-light melatonin onset (DLMO), is impractical for large-scale studies, and blood-based molecular biomarkers, while promising, are limited in feasibility. To address these challenges, we developed HairTime, a noninvasive assay that estimates circadian phase from a single daytime hair sample. Developed and evaluated in two steps—a training and a validation study—HairTime demonstrated strong predictive power compared to DLMO. Suitable for large-scale studies, it was assessed using over 4,000 samples. Circadian phase estimations showed a normal distribution and were associated with age, sex, and notably, work schedules, with earlier timing on workdays, suggesting that societal factors can modulate internal rhythms. Together, these findings establish HairTime as a promising tool for assessing circadian phase in research and lay the foundation for future applications in personalized chronotherapy.

circadian | chronotype | biomarker | clock | hair

Significance

Circadian timing varies widely among individuals, influencing sleep, behavior, and health. However, assessing individual circadian phase outside laboratory settings remains difficult because gold-standard methods such as dim-light melatonin onset (DLMO) are invasive and time-consuming. We developed HairTime, a simple, noninvasive assay that estimates circadian phase from a single hair sample. In an independent validation study, HairTime closely matched DLMO estimates. Applied to more than 4,000 individuals, HairTime revealed age-, sex-, and work schedule–related patterns consistent with established behavioral and physiological data. These results demonstrate that HairTime enables large-scale, population-level circadian assessment and provides a promising foundation for future clinical applications.

Human daily behavior is regulated by an endogenous timekeeping system known as the circadian clock. A genetic program is present in nearly all human cells, where individual cellular oscillators form networks that collectively constitute the circadian system. As a result, daily rhythms occur at the cellular, organ, and whole-organism levels. The circadian system orchestrates physiological and behavioral processes with respect to time of day and uses environmental cyclic cues, known as zeitgebers, to synchronize the body's internal time with the external environment—a process called entrainment. In mammals, the principal pacemaker, or central clock, is located in the suprachiasmatic nucleus (SCN) in the hypothalamus. The SCN is primarily entrained by the light–dark cycle and transmits time-of-day information to oscillators in peripheral tissues (1, 2). Through entrainment, circadian rhythms establish specific phase relationships with external zeitgeber cycles, known as phases of entrainment. In humans, there is considerable individual variation in these phases of entrainment, leading to interindividual differences in the timing of clock-controlled functions such as hormone secretion, alertness, cognitive performance, and physical activity. The sleep–wake cycle is one of the most prominent physiological processes governed by the circadian system. These individual differences in phase of entrainment are often referred to as chronotype and are most evident in sleep patterns, where some individuals have naturally earlier sleep times ("larks") while others are later ("owls"). Traditionally, chronotype has been assessed using questionnaires such as the Munich ChronoType Questionnaire (MCTQ) and the Morningness-Eveningness Questionnaire (MEQ) (3, 4). However, in the literature, the term chronotype is applied inconsistently: in some studies, it refers to a stable, trait-like characteristic, while in others it is used synonymously with the actual phase of entrainment. To avoid this ambiguity, in this paper we do not use the term chronotype, and instead focus on circadian phase, defined by biomarker-based measures such as dim-light melatonin onset (DLMO) (i.e., the point at which the pineal gland begins melatonin production in the absence of light). Since melatonin secretion is predominantly regulated by the SCN, DLMO serves as a reliable marker for the onset of the biological night (5).

Despite recent advances, the crucial interplay between the circadian clock and health remains largely underutilized in medical education and practice. For instance, disease

Competing interest statement: B.M. and A.K. are shareholders of BodyClock Technologies GmbH, which provided data for this study. The company's business model is based on intellectual property described in this publication. All other authors declare that they have no competing financial or personal interests that could have influenced the research presented in this article.

This article is a PNAS Direct Submission. R.A. is a guest editor invited by the Editorial Board.

[1]B.M., L.K.P., and S.Ö. contributed equally to this work.

[2]Present address: Department of Radiology, Weill Cornell Medical College, New York, NY 10065.

[3]To whom correspondence may be addressed. Email: achim.kramer@charite.de.

This article contains supporting information online at https://www.pnas.org/lookup/suppl/doi:10.1073/pnas.2514928123/-/DCSupplemental.

Published March 25, 2026.

symptoms, such as those experienced in asthma (6), follow distinct daily patterns. Similarly, medical emergencies, such as heart attacks (7, 8), also exhibit daily variation. Additionally, many genes encoding druggable proteins exhibit cyclic transcription in at least one tissue in primates (9). Yet, circadian timing is rarely considered in drug development, even though studies suggest that aligning treatments with biological rhythms can enhance effectiveness and reduce side effects (10, 11). A new field, circadian medicine (or chronomedicine), is now emerging to bridge this gap. It aims to uncover the mechanisms linking the circadian clock to health and disease and apply this knowledge to improve diagnosis, treatment, and prevention.

Circadian precision medicine aims to optimize treatment by aligning medical interventions with an individual's biological rhythms. Since people vary in their circadian phase, the assessment of internal time is crucial for maximizing the benefits of circadian medicine. The current gold standard for estimating circadian phase, DLMO, is labor-intensive and requires multiple saliva or blood samples collected in the evening under controlled low-light conditions (12). These constraints make DLMO assessment impractical for large-scale studies and routine clinical applications. To circumvent these challenges, self-reported questionnaires such as the MCTQ and the MEQ are commonly used. The MCTQ estimates circadian phase based on reported sleep–wake times, while the MEQ assesses individual preferences for daily activities and self-perceived states (e.g., alertness, tiredness, cognitive, and mental performance) at different times of day. However, both rely on subjective self-assessment, which introduces potential biases. Several factors beyond the circadian clock may influence questionnaire-based circadian phase estimates. For instance, individuals with extreme sleep–wake patterns who struggle with rigid societal schedules may report their preferred timing on the MEQ reflecting their wish to have more moderate patterns. Similarly, MCTQ-based estimates can be affected by sleep homeostasis factors, such as sleep debt, despite computational adjustments designed to minimize this influence (13–15).

Gene expression in peripheral tissues can serve as a marker of the human circadian clock's phase and function (16–19), as the molecular clock machinery driving endogenous rhythms is present in almost all tissues (2, 9) and is synchronized by the SCN. Recently, several research groups have developed more feasible objective molecular biomarker tests that require only a single or a few blood or tissue samples. These advancements may enable objective circadian phase determination in larger cohorts (20, 21). We developed BodyTime, an assay that estimates internal time from a single blood sample using a small set of transcript biomarkers (22). Compared to DLMO, BodyTime demonstrated a strong performance while offering several advantages: i) Simpler integration into study protocols and clinical settings; ii) Lower cost and reduced logistical constraints (e.g., no need for controlled conditions during sample collection); iii) Objective measurement, avoiding the subjectivity of self-reported questionnaires. However, BodyTime has technical challenges that limit its scalability, particularly in large-scale studies and field research. The requirement to keep blood cells cold and isolate monocytes makes its widespread application difficult. To address these limitations, hair follicle cells were identified as a promising, less invasive alternative biospecimen. In these cells, clock gene expression follows a daily rhythm, with its phase aligning with behavioral rhythms (23). Additionally, because hair follicle cells remain attached to plucked hairs, no cell separation is required, and the RNA yield from a few plucked hairs is sufficient for standard gene expression analysis (24). A hair-based assay would facilitate internal time assessment in large-scale and field studies, enable longer follow-up periods for study participants and outpatients, and allow for more frequent sampling in longitudinal studies.

The phase of entrainment reflects the *state* of alignment between the endogenous circadian clock and the environmental zeitgeber cycle. While genetic variation helps explain why individuals synchronize differently to the same light–dark cycle, phase of entrainment also depends on zeitgeber strength (25). For instance, when individuals transition from urban environments to natural settings—where daylight exposure is high during the day and minimal at night—their phase of entrainment shifts significantly earlier demonstrating the plasticity of circadian phase (26). Yet, the extent to which circadian phase varies within individuals in response to environmental influences—such as seasonal changes, weather conditions, or daily behaviors—remains largely unknown. A key limitation in addressing this question is the lack of practical methods for its longitudinal assessment in naturalistic studies. Previous findings suggest that shifts in DLMO can occur over even shorter timescales, with measurable delays on work-free days compared to workdays (27). In modern lifestyles, characterized by irregular light exposure and inconsistent mealtimes, understanding the stability of circadian phase is crucial, not only for circadian research but also for personalized circadian medicine and preventive strategies.

In this study, we developed an assay (HairTime) to estimate circadian phase from hair samples collected at a single time point and validated it against the gold-standard marker, DLMO. Compared to blood sampling, hair collection is minimally invasive and does not require a healthcare professional—participants can collect their own samples and mail them in. This makes the assay easy to implement, cost-effective, and well-suited for large-scale studies and longitudinal assessments. Using data from a field sample of more than 4,000 individuals, we validated its ability to capture circadian phase at the population level. The data reproduced established associations with age and sex, and even the subtler effects of work schedules, known from questionnaire-based studies. These findings suggest HairTime as a robust tool for large-scale circadian research and highlight its promising role for future clinical application.

Results

To identify genes that are expressed in human hair roots in a time-of-day-dependent manner, we first performed a pilot study with three healthy volunteers. The objective was to identify rhythmic candidate genes in a small cohort, which could then be used in a larger study to build a training dataset for prediction of circadian phase from a single sample, without the necessity of analyzing all genes in the second study. The test subjects pulled out some of their own hair from the scalp at regular 4-h intervals over a period of 36 h. The RNA from the hair root cells was extracted, and the gene expression was analyzed by RNA sequencing. A total of 90 genes that exhibited consistent rhythmic activity were selected (Dataset S1).

To generate a training dataset, we conducted the *HairTime* study, in which we analyzed the gene expression of the 90 selected genes in conjunction with six housekeeping genes in 13 healthy male and female volunteers using a 96-plex NanoString panel (*SI Appendix*, Table S1 and S2). The volunteers were instructed to sample their hair roots at regular 3-h intervals over a 33-h period (Fig. 1*A*). To timestamp these data with respect to the individual's internal time, we also determined the DLMO from saliva samples of each participant on the second day of the study. This enabled us to describe the gene expression of the 90 candidate genes as a function of internal time (Fig. 1*B* and Dataset S2).

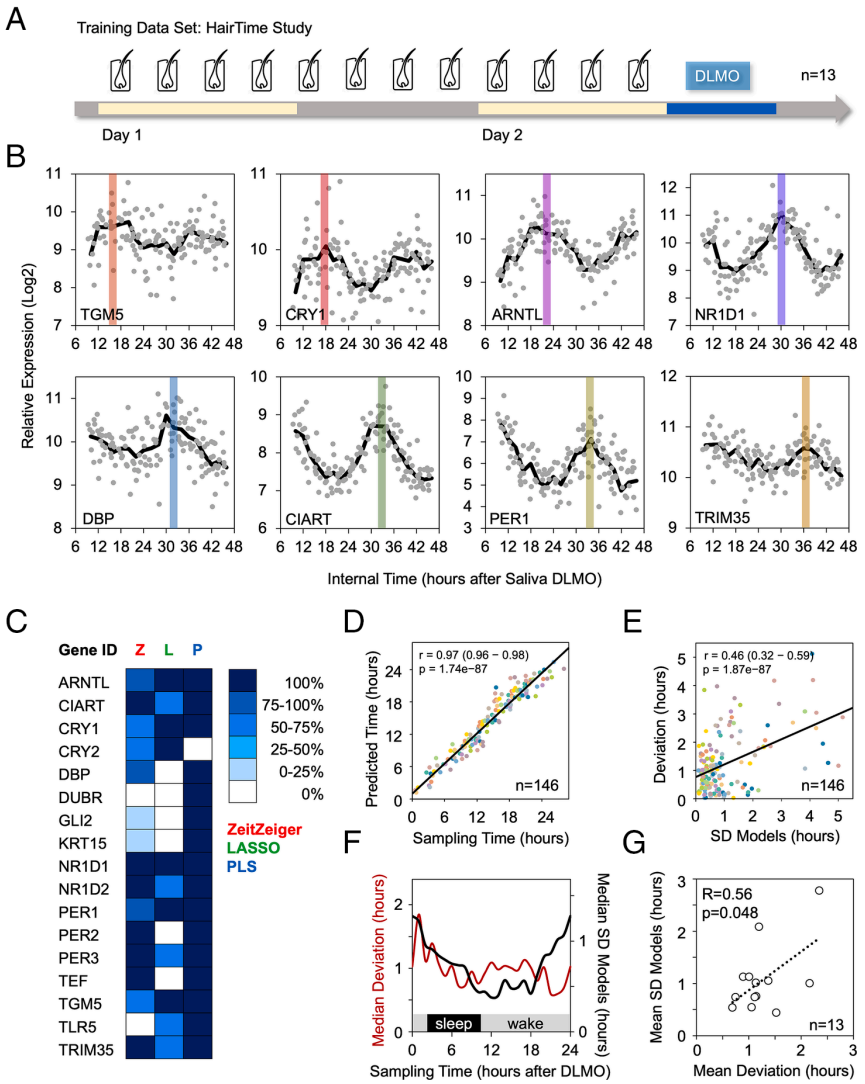

Fig. 1. Identification of transcriptional biomarkers from hair roots for prediction of human circadian phase. (*A*) HairTime study setup. (*B*) Composite expression rhythms of the indicated genes from the hair root samples of all 13 participants in the HairTime study. The black line represents 2-h bin mean values. The colored bars indicate the peak expressions of the genes. (*C*) Selected features (genes) and their relative frequency of occurrence in the different parameter versions of the ZeitZeiger, least absolute shrinkage and selection operator (LASSO), and partial least squares (PLS) models. (*D*) Repeated measures correlation (effective sample size corresponds to the number of individuals; n_subjects = 13; n_observations = 146) between the observed and the predicted internal time (mean of the three model predictions) from cross-validation approaches described in Methods. Dots are color-coded according to subject. (*E*) Repeated measures correlation between the degree of model disagreement (models SD) and the deviation of the hair prediction from the saliva DLMO-based internal time. Dots are color-coded according to subject. (*F*) Prediction accuracy and model agreement as a function of sampling time (given in hourly bins). Prediction accuracy is given as median deviation from saliva DLMO-based internal time for all samples per bin. Model disagreement is given as median of the SD of model predictions per bin. (*G*) Pearson's correlation between mean deviation of the predictions from saliva DLMO-based internal time and the disagreement of the models (given as mean SD of models) per study participant.

Because participants contributed multiple samples, effective sample size corresponds to the number of individuals rather than total hair samples.

To identify the most effective genes for predicting internal time (hours past DLMO) from a single sample, we applied three machine learning methods—ZeitZeiger, LASSO, and PLS—with cross-validation approaches as described in Methods. For each method, two models were retained based on cross-validation performance and feature selection. Internal time predictions were then averaged across the three approaches to obtain a final ensemble estimate. In total, 17 genes were identified for internal time prediction (Fig. 1*C* and Dataset S3).

While the prediction accuracy was remarkably high [median absolute deviation (MdAE) from saliva DLMO-based internal time of approximately 1 h, Fig. 1*D*], nearly 20% of samples in the training dataset exhibited a prediction deviation of more than 2 h. Interestingly, in these samples, the three prediction models frequently did not agree. Indeed, the SD of the three predictions demonstrated a highly significant association with the difference between the average model prediction and the saliva DLMO-based internal time (Fig. 1*E*) based on repeated-measures correlation to account for within-participant clustering. Consequently, the SD of the model predictions should allow estimation of prediction accuracy for future, hitherto unknown samples.

What factors contributed to the discrepancy in predictive accuracy across samples? To explore potential causes, we conducted a detailed analysis to assess whether prediction accuracy varied by time of day and whether there were notable interindividual differences among participants. Indeed, the prediction models exhibited considerable inconsistencies when using samples collected between approximately 4 h before and 8 h after DLMO (i.e., during the evening and nighttime), and were particularly inaccurate when

performed on nighttime samples (Fig. 1*F*). Moreover, we observed substantial interindividual differences in mean prediction accuracy, which correlated significantly with the mean SD of the prediction models across all samples from a given individual (Fig. 1*G*). This provides further support for the hypothesis that discrepancies between prediction models may serve as an indicator of accuracy.

Why does prediction accuracy vary between individuals? We hypothesized that this could be linked to the amplitude of their gene expression rhythms. This assumption is plausible, as lower amplitudes in noisy expression data are expected to increase susceptibility to errors in prediction models and lead to greater inconsistencies between models using different approaches. To test this hypothesis, we analyzed the amplitude of gene expression rhythms for each study participant. As a result of the significant positive correlation between the amplitudes of numerous gene expression rhythms (Fig. 2 *A* and *B*), an amplitude score was developed as an indicator of the amplitude of the circadian clock machinery in hair root cells. This score was derived from the five genes that exhibited the highest amplitude and strongest cross-correlation (*CIART*, *NR1D1*, *NR1D2*, *PER3*, *TEF*). Indeed, individuals with lower amplitude scores demonstrated a significantly lower degree of agreement between the predictions of the three models (Fig. 2*C*). This finding suggests that the accuracy of circadian phase prediction from a single biospecimen is dependent on the strength of a person's circadian system.

It is frequently observed that predictors demonstrate superior performance on datasets on which they were constructed than on independent samples. Consequently, it is critical to validate them externally prior to implementation for clinical or research purposes. Thus, to validate the final predictors, an independent study (*HairVali* study) with 35 healthy male and female volunteers was

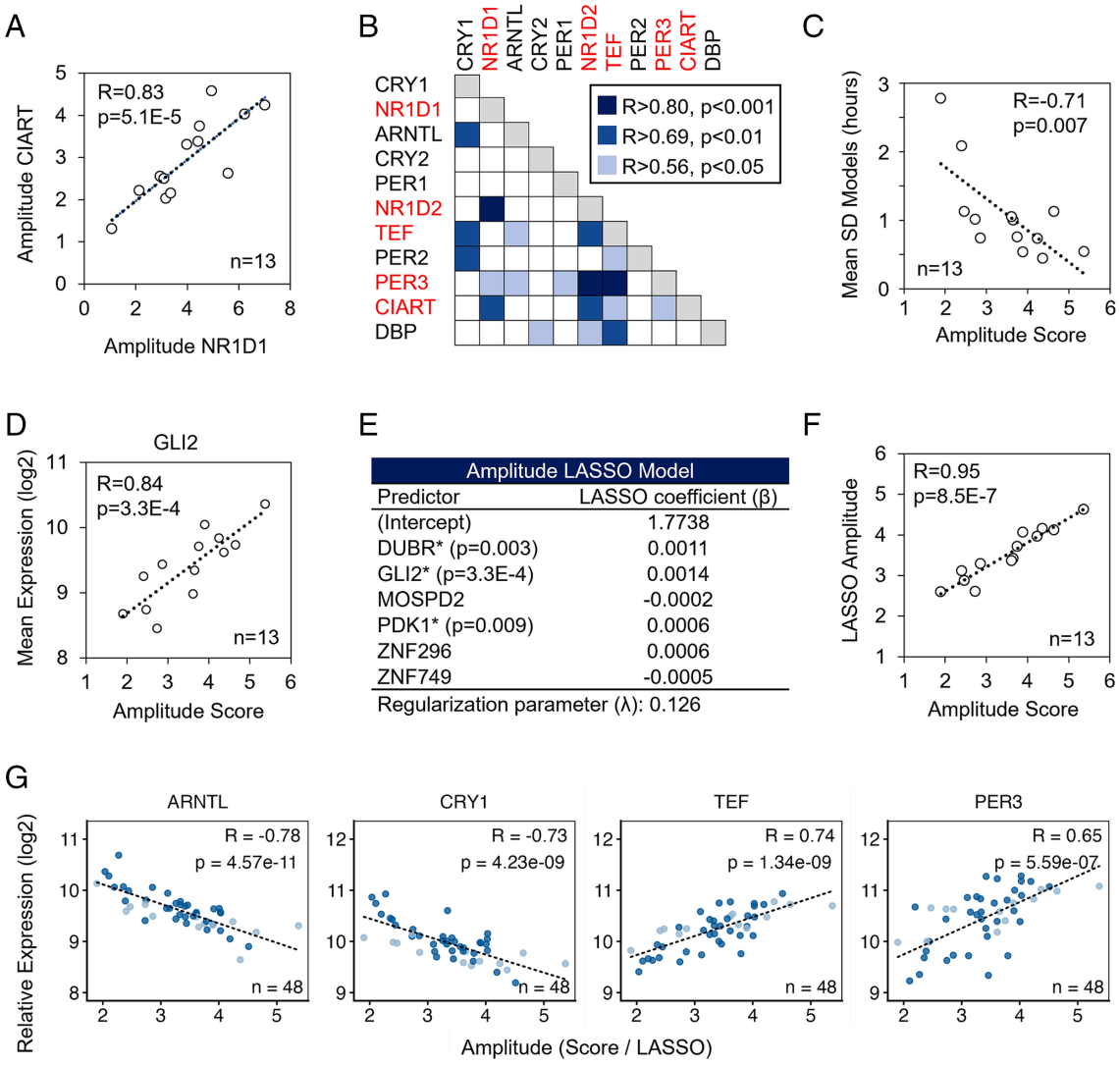

Fig. 2. Prediction of circadian amplitude using transcriptional biomarkers. (*A*) Pearson's correlation between rhythmic expression amplitudes of *NR1D1* and *CIART*, as an example, in the 13 HairTime study participants. (*B*) Pairwise Pearson's correlation between the amplitudes of the expression rhythms of the indicated genes (red: strongest cross-correlation). (*C*) Pearson's correlation between the amplitude score, calculated as the geometric mean of the expression rhythm amplitudes of the genes indicated in red in (*B*), and the mean model disagreement for each HairTime study participant. (*D*) Pearson's correlation between the amplitude score and the mean expression of the gene GLI2. (*E*) LASSO model coefficients (β) for predicting circadian amplitude derived from nonrhythmic candidate genes (main text and Dataset S4). Regularization parameter λ was adjusted to limit the number of predictive biomarkers to a maximum of six. Expression levels of genes marked with asterisks show significant correlations with the amplitude score [*P*-values indicated, example in panel (*D*)]. (*F*) Pearson's correlation between amplitude scores and predicted amplitudes from LASSO model shown in (*E*). (*G*) Pearson's correlation between gene expression level and amplitude. Dark points indicate participants with a single expression measurement (HairVali), whereas light points indicate participants with 4 to 5 measurements (HairTime, expression averaged within participant). The reported Pearson correlation coefficients and *P*-values are based on the subject-level data and n represents the number of participants.

conducted (*SI Appendix*, Table S1). The saliva DLMO and the expression of the 17 prediction genes determined in the HairTime study (Fig. 1*C*) from a single hair root sample taken between 9 and 17 h after DLMO (i.e., between morning and early afternoon) were determined (Fig. 3*A*). In this independent dataset, the prediction accuracy of DLMO from hair root gene expression using the three models was again remarkably high, with a combined MdAE of 0.99 h and more than 77% of all samples exhibiting a prediction deviation of less than 2 h (Table 1 and Fig. 3*B*). However, some samples exhibited markedly lower agreement between model-predicted and saliva-measured DLMO, prompting us to investigate potential causes. As in the training dataset, we observed a significant correlation between the deviation of predicted from measured DLMO and the degree of disagreement among the three model predictions (Fig. 3*C*). In other words, the more the individual models diverged from each other, the larger the deviation of the predicted from the measured DLMO tended to be. In our HairTime study, such model disagreement was found to correlate with lower circadian amplitude (Fig. 2*C*), suggesting that samples with large differences between observed and predicted DLMO (pDLMO) may originate from individuals with weaker circadian rhythmicity.

To measure amplitude, time series data from individuals are required, as this parameter cannot yet be estimated from a single sample. To address this limitation, we systematically searched our training data for genes whose absolute expression levels might reflect individual amplitude, as previously reported in mouse models (28). We observed that the expression levels of certain individual genes correlated with measured amplitude in hair root cells (Fig. 2*D*), suggesting that gene expression may contain information relevant to interindividual amplitude differences. Based on this observation, we applied LASSO regression to predict circadian amplitude in hair root cells from gene expression levels measured between morning and noon. To reduce the influence of temporal variation, we focused on the 46 most stable genes from our 90-gene panel (Dataset S4). The resulting model identified six genes (*DUBR*, *GLI2*, *MOSPD2*, *PDK1*, *ZNF296*, and *ZNF749*) as informative predictors of amplitude in hair root cells (Fig. 2*E*). Predicted amplitude values were significantly correlated with measured values in the training data (Fig. 2*F*). We then applied this model to estimate amplitude in the independent HairVali cohort; however, these estimates should be considered exploratory, as independent validation has not yet been performed.

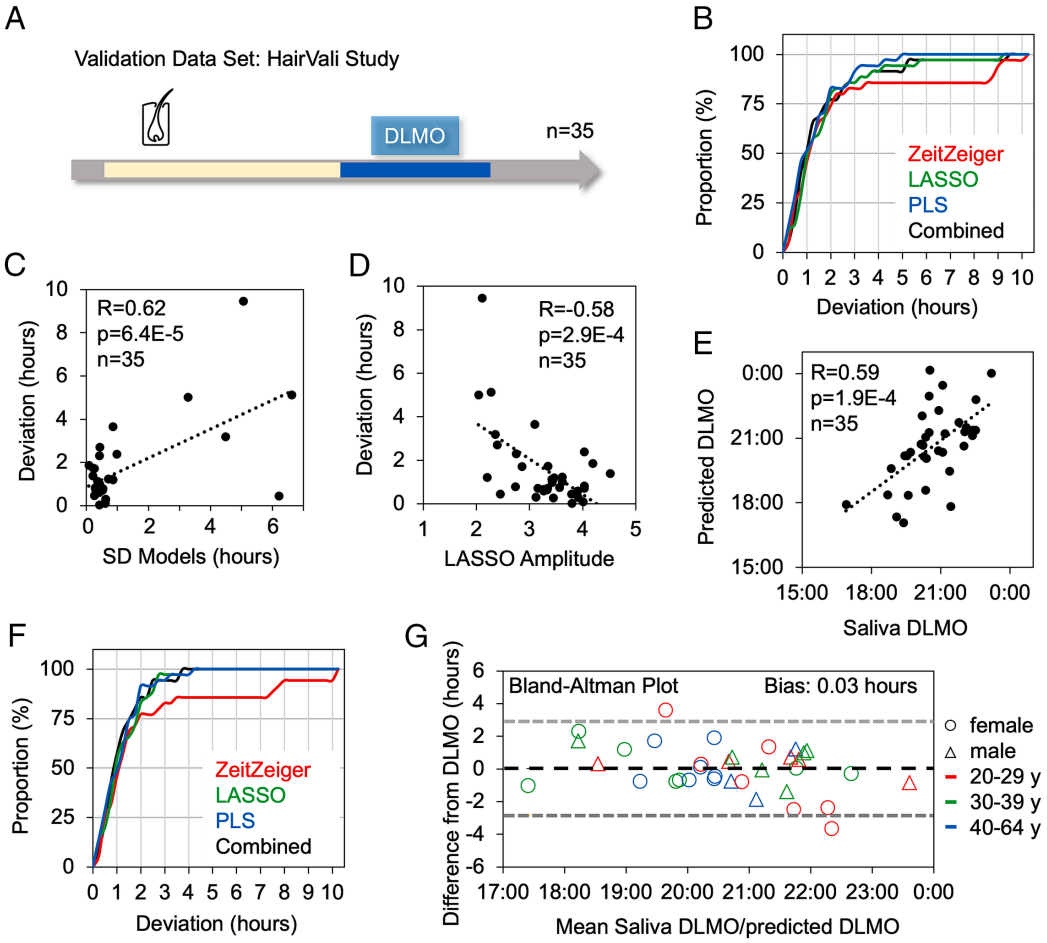

Fig. 3. Validation of biomarkers for prediction of human circadian phase in an independent study. (*A*) HairVali study setup. (*B*) Cumulative frequency distributions of the absolute prediction deviation from saliva DLMO values for three different models and their mean (combined) when applied to the HairVali study dataset. (*C*) Pearson's correlation between model disagreement and deviation from saliva DLMO values for samples of the HairVali study. (*D*) Pearson's correlation between the LASSO-predicted amplitude of the circadian system of participants in the HairVali study and the deviation of the pDLMO from the saliva DLMO value. (*E*) Pearson's correlation between saliva DLMO and DLMO predicted from hair root biomarkers for HairVali study samples. Gene expression values of six low-amplitude samples (LASSO amplitude < 2.4) were adjusted as described in the main text and in the Materials and Methods section. (*F*) Cumulative frequency distributions of the absolute prediction deviation from saliva DLMO values for three different models and their mean (combined) when applied to the HairVali study dataset after adjustment of low-amplitude samples. (*G*) Bland–Altman analysis of the bias between saliva DLMO and DLMO predicted (difference = saliva − predicted) from hair root biomarkers (combined, i.e., average of the three prediction models). The black dashed line corresponds to mean difference between methods; gray dashed lines correspond to the limits of agreement (mean difference ± 1.96 SD).

Table 1. External validation of the HairTime predictors in the independent HairVali study

Predictor	Type of validation sample	Absolute prediction error [h] median [IQR]	Absolute prediction error ≤ 1 h [% of samples]	Absolute prediction error ≤ 2 h [% of samples]
ZeitZeiger	All (n = 35)	1.13 [1.48]	45.7	74.3
LASSO	All (n = 35)	1.08 [1.07]	48.6	80.0
PLS	All (n = 35)	0.80 [1.39]	51.4	82.9
Combined*	All (n = 35)	0.99 [1.17]	51.4	77.1
Combined*	High amp (n = 29)	0.76 [0.64]	62.1	89.7
Combined*	All, low amp adjusted (n = 35)†	0.80 [0.95]	57.1	85.7

*Combined: Circular mean of ZeitZeiger, LASSO, and PLS predictions.
†Secondary, exploratory analysis.

Utilizing this amplitude prediction model, we calculated amplitude scores for the 35 HairVali participants, which ranged from 2.0 to 4.5 [mean 3.3, 95% CI (3.05; 3.50)]. This is analogous to the observations made for the 13 HairTime participants, for whom the range was 1.9 to 5.4 [mean 3.5, 95% CI (2.92; 4.41)]. As anticipated, the prediction accuracy of the 35 HairVali samples exhibited a significant correlation with the amplitude scores derived from the model. The prediction error was higher for samples from participants with low amplitudes than for samples from participants with normal or high amplitudes (Fig. 3*D*). Subsequently, the accuracy of our phase prediction was analyzed without the samples from subjects with low amplitude (6 out of 35). The resulting MdAE was 0.76 h, with 90% of all samples exhibiting less than a 2-h deviation and 62% of all samples deviating by less than an hour from the measured DLMO (Table 1).

Although amplitude prediction can be used to identify samples whose phase prediction is likely to be less accurate, our next objective was to obtain more accurate phase prediction for low-amplitude samples. In our previous study with septic shock patients (29), we observed that the amplitudes of the clock gene expression rhythms were markedly low, and that the absolute mean expression levels of these genes were frequently significantly altered. We thus sought to determine whether such an association could also be identified in our healthy subjects. Indeed, a significant positive correlation was identified between amplitude and mean expression level for nine of the 17 phase prediction genes (*CIART*, *CRY2*, *DBP*, *NR1D2*, *PER1*, *PER2*, *PER3*, *TEF*, and *TRIM35*) (Fig. 2*G*). To account for this relationship, the gene expression values of the six low-amplitude samples from the HairVali study were adjusted using the parameters derived from the linear regressions. This adjustment ensured that the expression values corresponded to those of a sample with a mean amplitude score of 3.5 (*Materials and Methods*). The application of these adjusted expression values to the phase prediction of the six previously described samples resulted in a notable improvement in accuracy and a significant correlation between the DLMO predicted using a single hair sample and the DLMO measured in saliva (Fig. 3*E*). Consequently, the overall prediction accuracy of the 35 samples (including the six adjusted) is MdAE = 0.80 h, with 86% of all samples having less than a 2-h deviation and 57% of all samples having less than an hour's deviation from the measured DLMO; the adjusted low-amplitude predictions are reported as a secondary, exploratory analysis (Fig. 3*F* and Table 1). In addition, Bland–Altman analysis reveals no systematic bias between the hair-based prediction and DLMO [mean difference 0.03 h, 95% CI (−2.84; 2.90)] (Fig. 3*G*). Bland–Altman analysis using a regression approach suggested proportional bias, primarily observed in the younger age group (*SI Appendix*, Fig. S1).

The combined results demonstrate that our objective test is capable of accurately predicting the internal phase from a single hair sample. Furthermore, the amplitude score and the application of three distinct models provide a means of estimating the accuracy of the prediction. In instances where the prediction is deemed to be inaccurate, the method allows for the correction of low-amplitude samples, thereby enhancing the precision of the phase prediction.

To characterize circadian phase predicted from hair in a larger cohort and assess whether the values align with known distributions and epidemiological patterns previously observed in the field, we analyzed data from the BodyClock dataset. Hair samples were successfully processed from 4,351 individuals between December 30, 2021, and June 21, 2024, with most participants located in Germany at the time of sampling. Sociodemographic and occupational data were available for a subset of the sample (n = 4,044). We excluded individuals younger than 18 or older than 70, as these age groups were underrepresented and less likely to yield reliable estimates, resulting in a final sample size of n = 3,949 for analyses examining associations between age, sex, and work status with hair-based DLMO predictions. See *SI Appendix*, Table S3 for characteristics of each dataset.

The distribution of hair follicle–pDLMO was visually assessed and found to be approximately normal, with most participants clustering around 20:30 (Fig. 4*A*). A nonlinear association with age was observed, with younger individuals displayed later circadian timing compared to older individuals (Fig. 4*B*), consistent with previous findings using melatonin measurements of circadian phase (30). In addition, males exhibited slightly later pDLMO than females (Fig. 4*C*). This sex difference was further supported by the model that additionally included age (Fig. 4 *C*, *Inset* plot), suggesting an average difference of approximately 6 min.

To investigate whether hair-based circadian phase assessments reflect lifestyle-related differences, we conducted additional analyses based on the post hoc hypothesis that the slightly later circadian phases observed in participants over 60 y old could be attributed to a higher proportion of nonworking individuals in that age group. As expected, participants who were occupationally active had an earlier pDLMO than those not working (Fig. 5*A*). Furthermore, participants who collected hair samples during the week (Wednesday/Thursday/ Friday) had an earlier pDLMO than those sampled on Sunday (Fig. 5*B*), suggesting a difference in phase of entrainment between weekdays and weekends. These findings were further supported by models adjusted for age and sex, which estimated that working individuals had a pDLMO approximately 34 min earlier than nonworking individuals, while weekday samples showed a pDLMO about 12 min earlier than those collected on Sundays (Fig. 5 *A* and *B*, *Insets*). Finally, the number of self-reported workdays per week was negatively correlated with pDLMO (Fig. 5*C*), with an earlier circadian phase observed among individuals working more days per week.

Discussion

We developed and validated HairTime, a simple and accurate test for determining human phase of entrainment, requiring only a few hair roots collected at a single time point during the day.

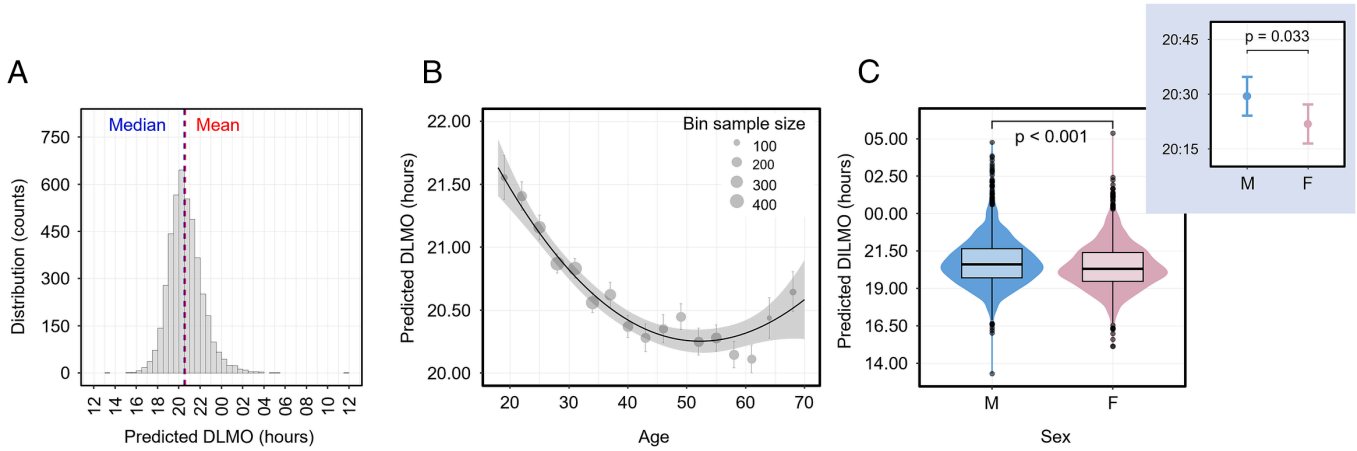

Fig. 4. Epidemiology of HairTime-based human circadian phase. (*A*) Distribution of pDLMO in the entire sample (n = 4,351). Circadian phase predicted from hair follicles is associated with age (*B*) and sex (*C*) (n = 3,949). In (*A*), the red dashed line represents the mean, and the blue dashed line represents the median. In (*B*), the line represents the fit from model, with sex and age as a spline term. The shaded area shows the 95% CI of the fit. Dots and whiskers represent pDLMO (raw data) mean ± SEM by age category. In (*C*), the main panel shows sex differences, where $P < 0.001$ according to *t* test. The inset depicts estimated marginal means and 95% CI from the model with age and sex as independent variables.

Methods like this, which can be scaled and integrated into clinical routines, are essential for advancing our understanding of circadian rhythms and their role in health and disease. Accurate assessments of circadian phase of entrainment are especially valuable for personalizing chronotherapy—helping determine the optimal timing for treatments or medications based on an individual's internal time. The current gold standard for assessing phase of entrainment, DLMO, is cumbersome, requiring multiple blood or saliva samples collected in a controlled environment across a broad window around bedtime. Previously, we developed the BodyTime assay, which predicts DLMO using a single blood sample, but its collection and processing limitations restricted its use to smaller, laboratory-based studies. In contrast, HairTime is minimally invasive and provides similarly accurate predictions in both training and validation sets, with a MdAE from saliva DLMO of less than 1 h. Over 85% of the samples showed deviations of less than 2 h. Our estimate of circadian phase is based on the average of predictions from three models—ZeitZeiger, LASSO, and PLS—and we demonstrate that the SD of the model predictions can serve as an approximation of accuracy. Higher SD between models correspond to poorer prediction accuracy. These machine learning models used selected molecular transcript biomarkers, many of which are genes associated with the core circadian oscillator (e.g., *PERs*, *CRYs*, *ARNTL*, *NR1Ds*). Several of these genes have also been identified as biomarkers in assays of circadian phase from other tissues, including blood. At the same time, we observed genes specific to hair follicle cells, suggesting that combining broadly expressed clock genes with tissue-specific output genes offers an optimal basis for accurate phase estimation.

Recent studies have explored various methods to estimate the phase of entrainment using a single or few biological samples, such as gene expression and metabolites in blood, or gene expression in skin (16, 19, 31–33). However, our study uses hair follicles collected at a single timepoint as a source for circadian phase estimation. Hair follicles offer several advantages as a biological material: they are more accessible, can be collected with minimal or no invasiveness, and are more stable than other samples like urine or blood. Moreover, hair samples are easier to store and transport, and their preparation is less expensive. Participants can collect hair samples in a stabilizing solution and easily mail them back at room temperature, making the process even more convenient for large-scale data collection. Our analysis, based on over 4,000 samples from the BodyClock dataset, demonstrates HairTime's feasibility and scalability for larger-scale studies.

Since the prediction accuracy of HairTime varied between subjects, we hypothesized that the amplitude of circadian transcript rhythms might partly explain this variability. Specifically, we assumed that phase predictions are likely to be less accurate when the amplitude is lower. To explore this, we developed an amplitude score based on the rhythms of five circadian genes: *CIART*, *TEF*, *NR1D1*, *NR1D2*, and *PER3*. These genes were chosen due to their high amplitude and strong cross-correlation in the HairTime training sample, with the latter three genes previously identified as key indicators of circadian properties in hair follicles (23). Interestingly, individuals with lower amplitude scores showed poorer agreement between the phase predictions of the three models in the training set. This finding supports our hypothesis that the accuracy of phase prediction is influenced by the strength of circadian rhythms in the hair follicle cells. To predict this amplitude score from a single timepoint, we identified six genes with minimal variation in expression throughout the day and trained a model to estimate amplitude based on their absolute expression levels in the morning. As expected, in the validation study, the predicted amplitude score correlated with the accuracy of circadian phase predictions.

The concept of circadian amplitude is not clearly defined, and there is no consensus on a gold standard for its assessment. Reduced amplitudes in rest-activity and skin temperature rhythms have been associated with aging and various diseases (34–36). While it is commonly assumed that this decline reflects changes in the endogenous circadian system, it remains unclear whether such reductions are governed by the circadian system itself or are influenced by external factors (20). Nonetheless, the amplitudes of melatonin, cortisol, and core body temperature respond similarly to interventions, suggesting they may reflect the amplitude of SCN oscillations (37). It is still unknown whether amplitude information derived from hair follicle cells can serve as a marker of the central clock's amplitude or if it primarily reflects that of local clocks. Given the multioscillator nature of the human circadian system, the amplitudes and phases in peripheral tissues may, under certain conditions, reflect either the rhythmicity imposed by the central clock or that of local clocks—an area that warrants further investigation. In this context, our amplitude prediction model based on a single hair sample should be viewed as an

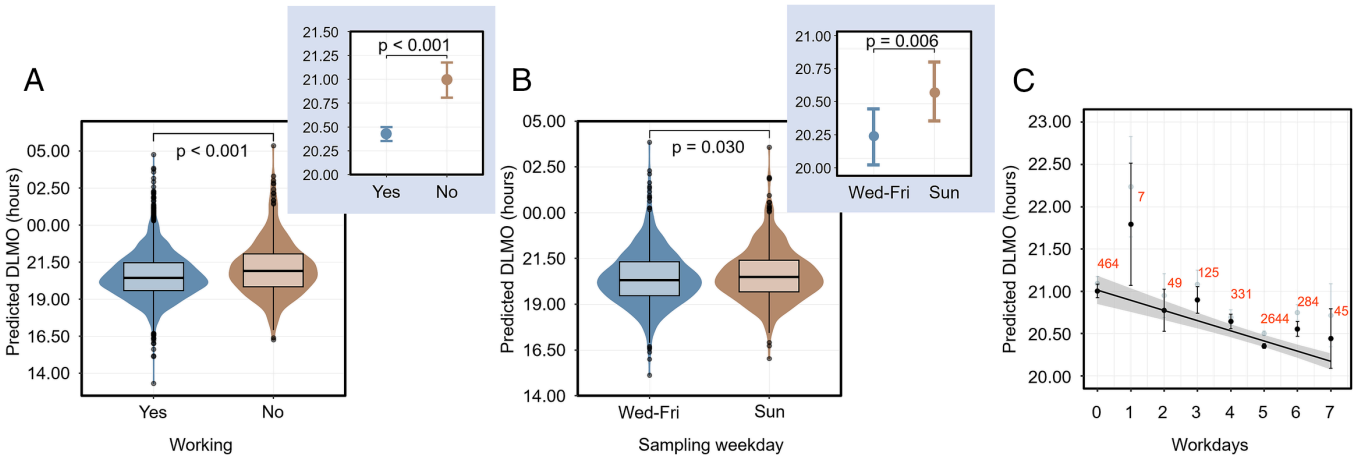

Fig. 5. Predicted circadian phase and work schedules. (*A*) pDLMO (circadian phase) is earlier among individuals who report being occupationally active compared to those who are not (n = 3,949, *t* test). The inset plot shows estimated marginal means and 95% CI from model adjusted for age and sex. (*B*) Circadian phase is also earlier when hair samples were collected on a weekday (Wednesday, Thursday, or Friday) compared to Sunday (n = 1,450, *t* test). The inset plot displays estimated marginal means and 95% CI from model, adjusted for age and sex. (*C*) A higher number of self-reported workdays per week is associated with earlier pDLMO (n = 3,949). The line represents the fit from linear model, adjusted for age and sex. Dots and whiskers show mean pDLMO ± SEM, with raw data in gray and adjusted values in black. Sample sizes for each category are indicated in orange.

exploratory, proof-of-concept approach to assess interindividual differences in local rhythmicity strength. Future studies will be required to validate this predictor, also against established systemic markers of circadian amplitude, such as melatonin or cortisol rhythms. Nevertheless, the model may already serve as a valuable tool for exploring interindividual differences in peripheral clock function and for tracking responses to interventions aimed at strengthening the circadian system, such as light therapy, melatonin, or time-restricted eating (38).

While our phase models were trained to predict DLMO, and thus the phase of the SCN, it remains unclear whether their accuracy is maintained when sleep patterns are displaced (e.g., in shift work or jetlag). For example, predictions of DLMO from activity and light exposure tend to be less accurate when individuals are misaligned (39). Mistimed sleep has been shown to affect the rhythmicity of circadian transcripts in whole blood samples (40), suggesting that expression profiles in peripheral tissues are not only influenced by the central circadian clock but also by external cues, such as temperature, nutrition, and those related to the sleep–wake cycles. Previous research showed that hair follicles phase correlate with the phase of behavior (i.e., sleep–wake, eating times). However, in an experiment where sleep–wake and eating times were advanced by 4 h over 3 wk in two subjects, along with high-intensity light exposure to adjust circadian rhythms, the phase shifts in hair follicle transcript rhythms were more closely aligned with those observed in salivary melatonin and cortisol than with those in sleep behavior (23). Additionally, the phase shifts in hair follicle rhythms were less drastic compared to activity rhythms in a small sample of rotating shift workers. Although very preliminary, these findings suggest that HairTime may not be highly susceptible to mistimed sleep and that even in challenging situations like sleep displacement, it may still provide relatively accurate estimates of circadian phase. Further studies are however needed to confirm whether HairTime still accurately reflects DLMO in misaligned conditions, which would set it as a valuable tool for assessing phase in conditions where the sleep–wake cycle is disrupted.

In the large BodyClock dataset, HairTime-derived estimates of circadian phase closely matched the distribution seen for DLMO, including its well-documented age dependency (30). In contrast to this robust age effect, evidence for sex differences in circadian phase remains inconsistent across studies. For example, while they may not be evident in DLMO and MEQ (30), men were slightly later when circadian phase was assessed using the MCTQ (4). Recent studies have suggested that questionnaire-based differences of phase of entrainment between men and women may be smaller than previously thought (41). Consistent with these findings, we observed that predictions of phase of entrainment from hair samples was slightly later in men. This suggests that HairTime can reliably capture age- and sex-related differences in phase of entrainment, similar to other established measures such as DLMO, but also offers the potential for large-scale epidemiological studies of circadian rhythms.

Interestingly, our exploratory analyses with the BodyClock dataset indicate that HairTime can also detect associations of lifestyle and environmental factors with circadian phase. For example, samples collected on weekends generally exhibited later circadian phases, whereas participants reporting more workdays tended to show earlier phases. These patterns are consistent with previous findings from both questionnaire-based assessments and DLMO studies. While BodyClock is a cross-sectional dataset and longitudinal shifts have not been directly measured, our results are compatible with the concept of circadian phase plasticity. HairTime can capture aspects of this dynamic variation, reflecting influences of environmental and behavioral factors such as work schedules, sleep patterns, mealtimes, and time spent outdoors or in front of screens.

A key question that remains is whether our results reflect genuine changes in the central clock, as opposed to behavior deviating from the circadian phase and influencing local gene expression. While phase shifts of the circadian system are a fundamental and well-established property, recent work has highlighted that, under real-world conditions, measurable changes in the phase of entrainment assessed by DLMO can be observed between workdays and work-free days, particularly in individuals with a later circadian phase as determined by the MCTQ (27). These findings highlight that circadian phase estimates derived from physiological output markers, such as DLMO, can vary over short timescales in response to everyday changes in sleep–wake behavior and light exposure. This raises the question of whether such variation reflects dynamic adjustments of circadian entrainment or differential sensitivity of output markers such as DLMO, while the central

oscillator itself remains comparatively stable. Relatedly, it remains to be determined whether the adverse health outcomes associated with social jetlag and irregular sleep timing primarily result from a constantly shifting internal clock or from behaviors that are constantly misaligned with a relatively stable clock. In either case, currently available evidence suggests that interventions should aim to stabilize both behavioral and internal rhythms to mitigate health risks (42–44). HairTime, in turn, may serve as a practical tool to quantify circadian phase in large samples and across time, allowing for future studies on how changes are associated with behavioral and health outcomes.

Our results should be interpreted in light of the study's strengths and limitations: i) HairTime was developed using a training set and validated on a separate validation set, demonstrating good accuracy compared to the gold standard, DLMO. The assay relies on fewer than 20 transcript biomarkers and combines three models to predict circadian phase, with the agreement between models serving as an indicator of accuracy. The six amplitude-associated genes were preselected based on temporal stability, but other potential masking factors, such as variable light or acute stress, were not tested. It should also be noted that the models were trained on a relatively small cohort, which may limit their generalizability. Additionally, the association between lower amplitudes and higher prediction error suggests that future studies should evaluate HairTime's accuracy in individuals with mistimed sleep in controlled settings (e.g., manipulated rest-activity rhythms). Further testing in men and women with diverse genetic backgrounds, as well as in relevant patient groups, is warranted. ii) Our analyses using the BodyClock dataset strongly support the applicability of HairTime in field studies, given the large sample size and the inclusion of various age groups and work characteristics. Although data were collected via convenience sampling and analyses were exploratory, we observed demographic patterns in hair-based phase of entrainment that align with those reported in the literature. Unfortunately, we lacked information on work start times, which could have provided a more complete understanding of the relationship between hair-based internal time and work schedules. Furthermore, inferences about the direction of causality are limited by our observational design. Our comparisons of weekdays vs. weekends were cross-sectional; despite controlling for age and sex and including only participants with five workdays per week, future studies using a within-subject design should further validate these findings.

In conclusion, HairTime is a pioneering, noninvasive assay that estimates the phase of entrainment by predicting DLMO from hair samples collected at a single time point, making it suitable for large-scale and field studies. Analyses in the large BodyClock cohort demonstrated that HairTime reproduces known associations of circadian phase with age, sex, and work-schedule at the population-level. Its feasibility is increased by the possibility of self-collection, combined with sample stability and ease of transport. Therefore, HairTime can be applied longitudinally to track individual circadian phase fluctuations over time. Taken together, these features highlight how HairTime holds promise for applications in circadian medicine, where aligning interventions with internal time may improve health outcomes.

Materials and Methods

Ethical Approval and Informed Consent. The studies in this paper were approved by the Ethics Committee of Charité–Universitätsmedizin Berlin (EA1/330/19 and EA4/200/19). All participants provided written informed consent prior to participation, acknowledging their voluntary involvement and understanding of the study procedures.

Pilot Study. Three healthy volunteers (two males, one female) collected hair follicle samples every 4 h over a period of 36 h (10 samples per donor). RNA was isolated from the samples, which were then sent for RNA sequencing (Novogene). Rhythmic gene expression was identified using MetaCycle (19). Genes were only included if at least 50% of the samples had an expression value of at least one for each of the three subjects resulting in 14,049 genes analyzed. Based on rhythmicity and amplitude, 90 candidate gene transcripts and six housekeeping gene transcripts were selected as potential time markers for the *HairTime* study. For details on sequencing quality, read numbers, and selection criteria, please refer to Dataset S1. Sleep–wake schedules were not controlled, as this pilot study aimed to identify candidate genes with potential rhythmic expression irrespective of circadian phase, whereas the HairTime study standardized schedules to enable precise phase modeling.

HairTime Study. This study aimed to identify transcript biomarkers in human hair follicles for predicting phase of entrainment. 13 healthy subjects were recruited (*SI Appendix*, Table S1) and trained on proper hair follicle sampling techniques. Participants were instructed to maintain a regular sleep–wake schedule for 7 d prior to sample collection, with compliance monitored using activity watches (Motion Watch 8, CamNtech) and sleep diaries. On day 8, participants collected 10 hair follicles every 3 h over a 33-h period (12 samples). 6 h before their habitual bedtime on day 9, participants visited the lab for melatonin saliva sampling at 30-min intervals. DLMO was determined as detailed below. RNA was isolated from hair samples, and gene expression was quantified as detailed below. The expression profiles of 96 genes (Dataset S2) were analyzed using the nCounter platform from NanoString. Because no prior data were available to inform power or sample size requirements for predictive modeling of circadian phase from hair samples, the study design and number of participants were guided by our previous successful work using 12 participants to develop a functional circadian assay (22). Of note, potential masking factors such as variable light exposure or acute stress were not explicitly controlled and may have influenced results.

HairVali Study. The aim of this study was to validate the transcript biomarkers identified in HairTime using an independent cohort. 35 healthy volunteers (*SI Appendix*, Table S1) were instructed to maintain a regular sleep–wake schedule for 7 d prior to sampling. On the morning of day 8, participants visited the lab to donate a hair follicle sample. In the evening of the same day, they returned to the lab 6 h before their usual bedtime for saliva sample collection to determine DLMO.

Hair Follicle Sampling. Participants were trained in hair follicle collection and asked to practice prior to starting. Briefly, they were instructed to grasp individual hairs or small strands with their fingers or tweezers and pull sharply in the direction of growth. After collection, participants visually confirmed that follicles had been extracted and placed them in collection tubes containing 1.5 mL RNAlater, prepared for each time point. Once the time series was completed, samples were transported to the lab on the same day and stored at 4 °C until further processing.

RNA isolation from hair follicles was performed using a TRIzol-based solid phase extraction method. Briefly, RNAlater solution was removed, and 800 μL of TRIzol was added directly to the tube containing the hair follicle sample. The sample was vortexed briefly and incubated for 5 min at room temperature. RNA was isolated following the protocol of the Direct-Zol RNA Micro Kit (Zymo Research). The RNA was then eluted in 10 μL of RNase-free water, stored on ice until quantification with the Qubit RNA Broad Range Assay Kit (Invitrogen), and stored at −80 °C for long-term preservation.

DLMO Assessment. Subjects entered a dimly lit room (<5 lx) 6 h before their habitual bedtime. Saliva samples were collected every 30 min (total of 12 samples per subject) using Salivettes (Sarstedt AG & Co.). The first sample was taken after 30 min under dim-light conditions, with the last sample collected at habitual bedtime. Eating and drinking were prohibited for 20 min prior to sampling. Upon collection, each sample was stored at –20 °C. Melatonin levels were measured using the Direct Saliva Melatonin Kit (BÜHLMANN). Circadian phase was determined by calculating the DLMO using the threshold method in Hockey-stick software (45), with a melatonin onset threshold of 3 pg/mL.

Quantification of Gene Expression. A custom 96-plex NanoString panel was designed, consisting of 90 candidate time-telling genes and six housekeeping genes (*SI Appendix*, Table S4). The probes included a 3′-biotinylated capture probe and a 5′-fluorescence-barcoded reporter probe for each target gene. This

panel was used in the HairTime and HairVali studies. Probe hybridization was performed with 400 ng of RNA from hair follicles, following the manufacturer's instructions. Raw expression data were obtained using the NanoString nCounter Digital Analyzer (NanoString Technologies). Counts were normalized to the housekeeping gene *CTLC* and log2-transformed for downstream analyses. A reduced panel of 24 time-telling, amplitude, and housekeeping genes was used to analyze samples from the BodyClock cohort (*SI Appendix*, Table S2).

Prediction of DLMO from Hair Follicle Gene Expression Panel. In a recent study, we applied three machine learning methods–LASSO, PLS, and ZeitZeiger (22, 46, 47)–to predict DLMO from transcriptome data of peripheral blood monocytes. In this study, we applied the same approach to hair follicle samples. Briefly, a training dataset was generated using gene expression data from the NanoString nCounter platform, collected in the HairTime study. These 13 time-series were time-stamped according to the individual time relative to DLMO. LASSO, PLS, and ZeitZeiger were then applied in the R statistical environment (48) to model internal time (hours after DLMO) and to guide feature discovery; details of model evaluation, cross-validation schemes, and feature selection are described in the subsequent section. The predicted value for "hours after DLMO" can be easily subtracted from sampling time to get "pDLMO" (in the unit that sampling time is represented, e.g., local time or standard time). Predictions were then averaged across the selected ZeitZeiger, LASSO, and PLS models. The circular mean of the three models was used as pDLMO unless stated otherwise. DLMO and pDLMO are clock-time variables, and linear calculations across midnight can produce artifacts. To avoid wrap-around effects, we consistently applied a "recentering" strategy: the 24-h clock is rotated so that the cut point (e.g., where 0 h meets 24 h) falls in a region with few or no observations. Because their distribution is unimodal and tightly clustered, this approach allows correct computation of averages, errors, and regression models. Circular means were used to combine predictions from the three models at the individual level to ensure consistency without requiring person-specific cut points.

Feature Discovery and NanoString Panel Construction. To derive a reduced and robust set of transcript biomarkers for a targeted NanoString panel, we applied a structured feature discovery workflow using the HairTime dataset. Three complementary machine learning approaches–ZeitZeiger, LASSO regression, and PLS–were used to explore predictors of internal time (hours after DLMO) and guide feature selection. ZeitZeiger models were trained using multiple parameter combinations and evaluated with both leave-one-subject-out and leave-one-sample-out cross-validation, while LASSO and PLS were evaluated using leave-one-sample-out cross-validation. For each approach, model parameters and features were selected based on cross-validation performance, with two models retained per method. Predictions from these retained models were averaged within each approach, and all genes included were retained as candidate features. Candidate feature sets from the three approaches were then combined using a consensus-based strategy, prioritizing genes present in at least two methods and restricting the final selection to fit a 24-plex NanoString panel. Predictions from the three approaches were further averaged to generate a final ensemble prediction of internal time. Dataset S3 provides a complete overview of parameter combinations, cross-validation performance, gene selection frequencies, and the final 24 genes.

Amplitude Score and Model Prediction. Using data from the HairVali study, the amplitude of the expression rhythms of 11 clock genes was determined by fitting a cosine function with a period of 24 h to expression values for each participant. Cross-correlations between these amplitudes were assessed using Pearson's correlation to identify genes with coherent rhythmicity. An amplitude score for each participant was then derived as an indicator of the overall strength of circadian clock gene oscillations in hair root cells. Specifically, this score represents the geometric mean of the fitted amplitudes of the five genes showing the highest amplitudes and strongest cross-correlations. Using LASSO regression and the HairTime training dataset, we modeled amplitude scores as the dependent variable, with gene expression levels measured in the morning (from 6:00 AM to 1:00 PM) as the independent variable. This analysis focused on the 46 genes with least variability in expression. Parameter λ was adjusted to limit the number of predictive biomarkers to a maximum of six. The predicted amplitude scores were then compared to the computed amplitude scores using Pearson's correlation.

HairTime and HairVali Study—Data Analysis. Correlation analyses were used to investigate the association between observed and predicted internal time in both HairTime (training set; repeated measures correlation) and HairVali (validation set; Pearson's correlation) studies. Internal time was derived from three different machine learning models (ZeitZeiger, LASSO, PLS). Gene expression values of six samples with low amplitude (LASSO amplitude score < 2.4) were adjusted to compute circadian time (DLMO) predictions in HairVali. Agreement between predicted and observed values was also tested using Bland–Altman analysis in HairVali. Model disagreement was computed as the SD of the three models in the HairTime training set. Correlation analyses were used to investigate associations between models' disagreement and internal time or circadian phase predictions' accuracy in both datasets. Sampling time influence on prediction was assessed using visual inspection: Median model disagreement (median SD of model predictions) and median prediction accuracy (deviation of predicted from observed internal time) were plotted by sampling time, depicted as time since the individual's observed DLMO. Pearson's correlations were used to test the association of amplitude score with model disagreement in HairTime and with prediction accuracy in HairVali. Cumulative frequency distributions were used to visualize the distribution of prediction deviation from the observed DLMO values (absolute difference) for three different models, as well as their mean (combined), with and without adjustments for low-amplitude samples. For correlation analyses in the training set that involved multiple assessments per subject, we used repeated measures correlation (49) to account for nonindependence of observations. To assess the extent to which the parallel slopes assumption was violated, we additionally tested mixed-effects linear regression models with either random intercepts only or both random intercepts and random slopes (50). We used Bayesian information criterion (BIC) to compare both forms and found smaller BIC values for models with random intercept only, indicating there is no strong violation of the parallel slopes assumption. Furthermore, the resulting regression line was similar across methods, as was the estimated strength of the association. We therefore show plots and results from the repeated measures correlation analyses. Correlations between gene expression and amplitude scores were tested using both HairTime and HairVali samples. Since expression levels were available across different timepoints in HairTime, these values were averaged within participant. The reported Pearson correlation coefficients and *P*-values for these analyses are calculated at the subject-level.

BodyClock Dataset—Preprocessing. The HairTime biomarkers described in this study have been patent-pending (EP20210217005) and licensed to BodyClock Technologies, a spin-off from Charité Universitätsmedizin Berlin. BodyClock offers the test in a self-sampling kit as a lifestyle product, which includes detailed instructions for hair follicle sampling. After sampling, customers are instructed to register their sample online and send it by mail to the Laboratory of Chronobiology at Charité. During registration, customers are asked to complete a brief online questionnaire about their sleep habits and occupational status (*SI Appendix*, Table S4). BodyClock shared the anonymized data for research purposes, ensuring their data are processed in accordance with applicable data protection laws. Between December 2021 and June 2024, this process resulted in the collection of the BodyClock dataset, an initial analysis of which is presented in this paper.

Data from questionnaires and assays were merged and preprocessed using R (v. 4.2.2), *tidyverse* [v. 1.1.2, (51)] and *janitor* (52). During the merging process, extra entries were removed using criteria based on the following: quality control annotations, proximity of questionnaire submission and hair sampling dates, and questionnaire data plausibility. This resulted in the removal of 108 extra assay entries and 311 questionnaire extra entries (with same id). The R code for the plots, tests, and model results, as well as assumptions checks (linearity, normality of residuals with Q–Q plots, and homoscedasticity with residual vs. fitted plots) and sensitivity analysis is available (see *Data, Materials, and Software Availability*).

Entries where the assay failed quality control were excluded when assessing the distribution of phase of entrainment ($n = 180$). For analyzing the association of the phase of entrainment with age, sex, and work, we included only subjects with reliable self-reported data on age and sex (excluding $n = 296$) and work (excluding $n = 11$). Data from participants younger than 18 or older than 70 were also excluded ($n = 95$) due to underrepresentation, which could yield unreliable results.

The self-reported date of hair sampling was used to investigate differences of phase of entrainment by weekday. We included only participants who collected their hair samples on Wednesday, Thursday, Friday, or Sunday (excluding n = 1,773). Additionally, we restricted the analysis to those who reported working 5 d a week (excluding n = 726). Our assumption was that most subjects working 5 d/wk work Monday through Friday and that transition days may carry residual effects of the weekend or the week.

Sample sizes for each analysis are provided in the results section and figure legends. *SI Appendix*, Fig. S2 shows the dataset sample sizes and exclusion counts.

BodyClock Dataset—Data Analysis. Given the nearly normal distribution of the phase of entrainment, we used *t* tests to examine the association between this marker and categorical variables (sex, work status, and weekdays vs. weekend) and Pearson's correlation to examine its association with age and workday. To assess their independent effects, we performed a multivariable regression (model A) with both age and sex. We then analyzed the influence of work status (yes vs. no) and weekday (weekday vs. weekend) using multivariable regressions (models B and C, respectively) adjusted for age and sex. Finally, we assessed whether the number of workdays was associated with phase of entrainment in a multivariable regression adjusted for age and sex (model D). As these analyses are exploratory, *P*-values should be interpreted as indicative only, and no formal conclusions regarding statistical significance are intended. All *t* tests, Pearson correlations, and regression models were conducted using stats package as a part of R (v. 4.2.2). To extract regression results, we used the package *jtools* [v. 2.3.0, (53)] and *ggeffects* [v. 1.7.1, (54)] to estimate marginal means (predicted values) for visualization. We used *ggplot2* [v. 3.5.1, (55)], *ggpubr* [v. 0.6.0, (56)] for plotting. For linear independent variables of interest in each model (i.e., age and workdays), we used BIC to compare two functional forms: linear and spline transformation using *splines::bs* [v. 4.4.2, (57)]. We opted to use BIC, a Bayesian approach, as it provides a balance between model fit and model complexity, penalizing models with more parameters and thus helping to prevent overfitting. The model with the lower BIC value was selected as the best fit, and the selected model is reported in each case. The R code for the plots, tests, and model results, as well as assumptions checks (linearity, normality of residuals with Q–Q plots, and homoscedasticity with residual vs. fitted plots) is available at [github.com/Chronomedicine/HairTime.git]. Sensitivity analyses using circular statistical approaches additionally confirmed the robustness of the results. All analyses should be considered exploratory, and the results should be interpreted accordingly.

Data, Materials, and Software Availability. R code for the plots, tests and model results, as well as assumptions checks (linearity, normality of residuals with Q–Q plots, and homoscedasticity with residual vs. fitted plots) and sensitivity analysis have been deposited in Github (58). Other data are included in the article and/or supporting information.

ACKNOWLEDGMENTS. We thank Theresa Keller for reviewing our code and text on methods/results of BodyClock analyses and Rogério Boff Borges for statistical advice. This study was in part funded by the German Research Foundation (Deutsche Forschungsgemeinschaft) grant 541063275–TRR 418.

Author affiliations: [a]Division of Chronobiology, Charité–Universitätsmedizin Berlin, Corporate Member of Freie Universität Berlin and Humboldt Universität zu Berlin, Berlin 10117, Germany; [b]Department of Anesthesiology and Intensive Care Medicine, Campus Charité Mitte and Campus Virchow-Klinikum, Charité–Universitätsmedizin Berlin, Corporate Member of Freie Universität Berlin and Humboldt-Universität zu Berlin, Berlin 10117, Germany; [c]Experimental and Clinical Research Center, Charité–Universitätsmedizin Berlin, Corporate Member of Freie Universität Berlin and Humboldt-Universität zu Berlin, Berlin 10117, Germany; [d]Institute of Physiology, Sleep Research and Clinical Chronobiology, Charité–Universitätsmedizin Berlin, Corporate Member of Freie Universität Berlin and Humboldt Universität zu Berlin, Berlin 10117, Germany; and [e]Clinic for Sleep & Chronomedicine, St. Hedwig Hospital, Berlin 10115, Germany

Author contributions: B.M., L.K.P., and A.K. designed research; B.M., L.K.P., S.Ö., A.R., A.N.A., J.d.Z., and A.K. performed research; B.M., L.K.P., A.R., D.K., and A.K. analyzed data; and B.M., L.K.P., and A.K. wrote the paper.

1. R. G. Foster, Sleep, circadian rhythms and health. *Interface Focus* **10**, 20190098 (2020).
2. J. S. Takahashi, Transcriptional architecture of the mammalian circadian clock. *Nat. Rev. Genet.* **18**, 164–179 (2017).
3. J. A. Horne, O. Ostberg, A self-assessment questionnaire to determine morningness-eveningness in human circadian rhythms. *Int. J. Chronobiol.* **4**, 97–110 (1976).
4. T. Roenneberg *et al.*, Epidemiology of the human circadian clock. *Sleep Med. Rev.* **11**, 429–438 (2007).
5. E. B. Klerman *et al.*, Keeping an eye on circadian time in clinical research and medicine. *Clin. Transl. Med.* **12**, e1131 (2022).
6. F. A. J. L. Scheer *et al.*, The endogenous circadian system worsens asthma at night independent of sleep and other daily behavioral or environmental cycles. *Proc. Natl. Acad. Sci. U.S.A.* **118**, e2018486118 (2021).
7. M. C. Cohen, K. M. Rohtla, C. E. Lavery, J. E. Muller, M. A. Mittleman, Meta-analysis of the morning excess of acute myocardial infarction and sudden cardiac death. *Am. J. Cardiol.* **79**, 1512–1516 (1997).
8. J. E. Muller *et al.*, Circadian variation in the frequency of onset of acute myocardial infarction. *N. Engl. J. Med.* **313**, 1315–1322 (1985).
9. L. S. Mure *et al.*, Diurnal transcriptome atlas of a primate across major neural and peripheral tissues. *Science* **359**, eaao0318 (2018).
10. M. Abusamak *et al.*, Chronotherapy in head and neck cancer: A systematic review and meta-analysis. *Int. J. Cancer* **156**, 1015–1032 (2025).
11. F. Pigazzani *et al.*, Effect of timed dosing of usual antihypertensives according to patient chronotype on cardiovascular outcomes: The Chronotype sub-study cohort of the Treatment in Morning versus Evening (TIME) study. *EClinicalMedicine* **72**, 102633 (2024).
12. J. M. Murray *et al.*, A protocol to determine circadian phase by at-home salivary dim light melatonin onset assessment. *J. Pineal Res.* **76**, e12994 (2024).
13. A. Adan *et al.*, Circadian typology: A comprehensive review. *Chronobiol. Int.* **29**, 1153–1175 (2012).
14. T. Roenneberg, Having trouble typing? What on earth is chronotype? *J. Biol. Rhythms* **30**, 487–491 (2015).
15. T. Roenneberg, L. K. Pilz, G. Zerbini, E. C. Winnebeck, Chronotype and social jetlag: A (self-) critical review. *Biology* **8**, 54 (2019).
16. R. Braun *et al.*, Universal method for robust detection of circadian state from gene expression. *Proc. Natl. Acad. Sci. U.S.A.* **115**, E9247–E9256 (2018).
17. R. Braun *et al.*, Reply to Laing et al.: Accurate prediction of circadian time across platforms. *Proc. Natl. Acad. Sci. U. S. A.* **116**, 5206–5208 (2019).
18. E. E. Laing, C. S. Möller-Levet, S. N. Archer, D.-J. Dijk, Universal and robust assessment of circadian time? *Proc. Natl. Acad. Sci. U.S.A.* **116**, 5205 (2019).
19. G. Wu *et al.*, Population-level rhythms in human skin with implications for circadian medicine. *Proc. Natl. Acad. Sci. U.S.A.* **115**, 12313–12318 (2018).
20. D.-J. Dijk, J. F. Duffy, Novel approaches for assessing circadian rhythmicity in humans: A review. *J. Biol. Rhythms* **35**, 421–438 (2020).
21. M. Münch, A. Kramer, Timing matters: New tools for personalized chronomedicine and circadian health. *Acta Physiol.* **227**, e13300 (2019).
22. N. Wittenbrink *et al.*, High-accuracy determination of internal circadian time from a single blood sample. *J. Clin. Invest.* **128**, 3826–3839 (2018).
23. M. Akashi *et al.*, Noninvasive method for assessing the human circadian clock using hair follicle cells. *Proc. Natl. Acad. Sci. U.S.A.* **107**, 15643–15648 (2010).
24. S. J. Kim *et al.*, Gene expression in head hair follicles plucked from men and women. *Ann. Clin. Lab. Sci.* **36**, 115–126 (2006).
25. A. E. Granada, G. Bordyugov, A. Kramer, H. Herzel, Human chronotypes from a theoretical perspective. *PLoS One* **8**, e59464 (2013).
26. K. P. Wright *et al.*, Entrainment of the human circadian clock to the natural light-dark cycle. *Curr. Biol.* **23**, 1554–1558 (2013).
27. G. Zerbini, E. C. Winnebeck, M. Merrow, Weekly, seasonal, and chronotype-dependent variation of dim-light melatonin onset. *J. Pineal Res.* **70**, e12723 (2021).
28. E. S. Littleton, M. L. Childress, M. L. Gosting, A. N. Jackson, S. Kojima, Genome-wide correlation analysis to identify amplitude regulators of circadian transcriptome output. *Sci. Rep.* **10**, 21839 (2020).
29. G. Lachmann *et al.*, Circadian rhythms in septic shock patients. *Ann. Intensive Care* **11**, 64 (2021).
30. D. J. Kennaway, The dim light melatonin onset across ages, methodologies, and sex and its relationship with morningness/eveningness. *Sleep* **46**, zsad033 (2023).
31. M. del Olmo *et al.*, Inter-layer and inter-subject variability of diurnal gene expression in human skin. *NAR Genom. Bioinform.* **4**, lqac097 (2022).
32. E. E. Laing *et al.*, Blood transcriptome based biomarkers for human circadian phase. *Elife* **6**, e20214 (2017).
33. T. Woelders *et al.*, Machine learning estimation of human body time using metabolomic profiling. *Proc. Natl. Acad. Sci. U.S.A.* **120**, e2212685120 (2023).
34. T. G. Brooks *et al.*, Diurnal rhythms of wrist temperature are associated with future disease risk in the UK Biobank. *Nat. Commun.* **14**, 5172 (2023).
35. H. Feng *et al.*, Association between accelerometer-measured amplitude of rest–activity rhythm and future health risk: A prospective cohort study of the UK Biobank. *Lancet Healthy Longev.* **4**, e200–e210 (2023).
36. E. S. Musiek *et al.*, Circadian rest-activity pattern changes in aging and preclinical Alzheimer disease. *JAMA Neurol.* **75**, 582 (2018).
37. D.-J. Dijk *et al.*, Amplitude reduction and phase shifts of melatonin, cortisol and other circadian rhythms after a gradual advance of sleep and light exposure in humans. *PLoS One* **7**, e30037 (2012).
38. A. Kramer *et al.*, Foundations of circadian medicine. *PLoS Biol.* **20**, e3001567 (2022).
39. L. S. Brown *et al.*, A classification approach to estimating human circadian phase under circadian alignment from actigraphy and photometry data. *J. Pineal Res.* **71**, e12745 (2021).
40. S. N. Archer *et al.*, Mistimed sleep disrupts circadian regulation of the human transcriptome. *Proc. Natl. Acad. Sci. U.S.A.* **111**, E682–E691 (2014).
41. C. Randler, J. Engelke, Gender differences in chronotype diminish with age: A meta-analysis based on morningness/chronotype questionnaires. *Chronobiol. Int.* **36**, 888–905 (2019).
42. S. L. Chellappa *et al.*, Daytime eating prevents internal circadian misalignment and glucose intolerance in night work. *Sci. Adv.* **7**, eabg9910 (2021).

43. N. De Sá Couto-Pereira *et al.*, Routine regularity during a global pandemic: Impact on mental health outcomes and influence of chronotype. *Chronobiol. Int.* **41**, 456–472 (2024).
44. T. L. Sletten *et al.*, The importance of sleep regularity: A consensus statement of the National Sleep Foundation sleep timing and variability panel. *Sleep Health* **9**, 801–820 (2023).
45. K. V. Danilenko, E. G. Verevkin, V. S. Antyufeev, A. Wirz-Justice, C. Cajochen, The hockey-stick method to estimate evening dim light melatonin onset (DLMO) in humans. *Chronobiol. Int.* **31**, 349–355 (2014).
46. J. Franklin, The elements of statistical learning: Data mining, inference and prediction. *Math. Intell.* **27**, 83–85 (2005).
47. J. J. Hughey, T. Hastie, A. J. Butte, ZeitZeiger: Supervised learning for high-dimensional data from an oscillatory system. *Nucleic Acids Res.* **44**, e80 (2016).
48. R Core Team, R: A language and environment for statistical computing, version 4.4.2 (R Foundation for Statistical Computing, Vienna, Austria, 2024).
49. J. Z. Bakdash, L. R. Marusich, Repeated measures correlation. *Front. Psychol.* **8**, 456 (2017).
50. D. Bates, M. Mächler, B. Bolker, S. Walker, Fitting linear mixed-effects models using lme4. *J. Stat. Softw.* **67**, 1–48 (2015).
51. H. Wickham, R. François, L. Henry, K. Müller, D. Vaughan, dplyr: A grammar of data manipulation, version 1.1.2. Comprehensive R Archive Network (CRAN) (2023). https://CRAN.R-project.org/package=dplyr. Accessed 22 February 2026.
52. S. Firke, Janitor: Simple tools for examining and cleaning dirty data, version 2.2.0. Comprehensive R Archive Network (CRAN) (2024). https://CRAN.R-project.org/package=janitor. Accessed 22 February 2026.
53. J. A. Long, Jtools: Analysis and presentation of social scientificdata. *J. Open Source Softw.* **9**, 6610 (2024).
54. D. Lüdecke, Ggeffects: Tidy data frames of marginal effects from regression models. *J. Open Source Softw.* **3**, 772 (2018).
55. H. Wickham, *ggplot2: Elegant Graphics for Data Analysis* (Springer, New York, 2009).
56. A. Kassambara, ggpubr: "ggplot2" based publication ready plots, version 0.6.0. Comprehensive R Archive Network (CRAN) (2023). https://CRAN.R-project.org/package=ggpubr. Accessed 22 February 2026.
57. D. M. Bates, W. N. Venables, R: B-spline basis for polynomial splines. (2021). https://stat.ethz.ch/R-manual/R-devel/library/splines/html/bs.html. Accessed 25 February 2025.
58. B. Maier *et al.*, HairTime analysis code. Zenodo. 10.5281/zenodo.18928125. Deposited 9 March 2026.